Natural Hazards (2020) 101:817–832
https://doi.org/10.1007/s11069-020-03897-x

ORIGINAL PAPER

Characteristics of a new regional seismic-intensity prediction equation for Spain

Julio Mezcua[1] · Juan Rueda[1,2,3] · Rosa M. García Blanco[3]

Received: 20 January 2020 / Accepted: 4 March 2020 / Published online: 11 March 2020

Abstract

An updated compilation of intensity files was performed based mainly on the most recent studies of earthquake intensity distribution in Spain [above all, the revision by Martínez Solares and Mezcua (Catálogo Sísmico de la Península Ibérica (800 a.C.-1900). Monografía No. 18, Instituto Geográfico Nacional, 2002)] and an intensity dataset generated by the Instituto Geográfico Nacional in 2008 using the *Did you feel it* Internet-based program. The large amount of data (more than 37,000 intensity data points) enabled us to calculate an intensity prediction equation for the whole of the Spanish mainland, as well as regional equations corresponding to three Spanish seismotectonic zones. The intensity prediction equations for the three different seismotectonic regions in the Iberian Peninsula (Betic, Stable Continental Region—SCR and Pyrenees) reflect their differences. The Pyrenees zone provides the highest maxima intensities for magnitudes M 5 and 6 in the 20–100 km range of hypocentral distance, but for that distance interval, the intensities for magnitude $M=4$ shown by the SCR region is higher. Finally, when comparing the theoretical intensity values obtained using the average intensity prediction equation for the Spanish mainland with the values in the dataset, anomalous behaviour occurs in the 60–120 km range, which can be explained by the Moho bounce of the energy that increases the corresponding intensity values in this distance range. This effect is suggested also by studying the PGV amplitude decay with distance using a set of 11 shallow events in the 4.5–5.1 moment magnitude interval.

Keywords Internet-based intensity · Spanish intensity attenuation · PGV and intensity distance behaviours · Moho-bounce effect

✉ Julio Mezcua
julio.mezcua@upm.es

[1] Fundación José García Siñeriz, Calle Alenza 1, 28003 Madrid, Spain

[2] Instituto Geográfico Nacional, Calle General Ibáñez de Ibero 3, 28003 Madrid, Spain

[3] Departamento de Ingeniería Topográfica Y Cartografía, ETSI Topografía, Geodesia y Cartografía, Universidad Politécnica de Madrid, Calle de la Arboleda s/n, 28031 Madrid, Spain

1 Introduction

In recent years, seismic intensity has emerged as an important parameter in seismological studies despite the lack of any simple relationship between this parameter and any of the other mechanical parameters that characterize earthquakes. This renewed interest has been highlighted by authors such as Bakun and Wentworth (1997), Gasperini et al. (1999), Atkinson and Wald (2007), Musson and Jiménez (2008), Hough (2013) and Atkinson et al. (2014), among others. The qualitative nature of seismic intensity weighs down heavily on their use in combination with other mechanical parameters of an earthquake. The vast increase in the quantity of data obtained by Internet-based methods of intensity determination means that this type of information can increasingly be employed, for example, in hazard studies (D'Amico and Albarello 2008; Mak and Schorlemmer 2016; White et al. 2018). In particular, the use of intensity in the attenuation of the crust, that is the energy propagated by destructive earthquakes known as the intensity prediction equation (IPE) of a determined area, is now habitually being used (López Casado et al. 2000; Bakun and Scotti 2006; Stromeyer and Grünthal 2009). Moreover, the performance of different IPEs, based on both Internet-derived and traditional data, is consistent, which implies that these two types of data are compatible, (Mak et al. 2015) and that their combined use may be able to increase resolution in the low intensity range (Hough 2013).

Intensity attenuation studies in Spain date back to Inglada (1921), who used Kövesligethy´s classic paper (Kövesligethy 1906) to obtain the focal depth of several earthquakes that occurred in Spain and the Ribatejo earthquake, Portugal, on 23 April 1909. Authors including Rey Pastor (1949), Romero and Bonelli (1951) and Bonelli and Esteban Carrasco (1957) calculated the IPEs of earthquakes based on the radius of isoseismal areas. However, the most recent attenuation studies carried out in Spain (e.g. Muñoz 1983; Martín 1984; López Casado et al. 2000; Mezcua et al. 2004; Goula et al. 2008; Stucchi et al. 2010; Gómez-Capera et al. 2015) are all related to the determination of seismic hazard and/or the regionalization of the intensity attenuation.

As mentioned above, the recent Internet-based gathering of intensity data has increased dramatically the available amount of intensity values and provides a more precise way of detecting regional changes in intensity attenuation and better definition of its behaviour at determined distances. Although no high-magnitude earthquakes have been felt recently in Spain (maximum magnitude of $M = 5.1$), the great number of intensity data points (IDP) collected with these new methods makes it possible to obtain new IPEs for Spain and for the different seismotectonic units on the Spanish mainland. The results obtained generate intensity prediction equations (IPE) for each region and for the whole of continental Spain. The use of IDPs to obtain the corresponding IPE means that you are considering the midpoint of each intensity class and the resulting intensity value at any distance is rounded off to the nearest integer value. This approach is different from that developed for obtaining the corresponding IPE from the isoseismal radii in which the estimated intensity values are truncated to the nearest integer (Musson 2005).

Another consequence of using a large number of IDPs in the construction of an IPE is that it enables us to detect small changes in the intensity distribution over distance, which, in turn, helps define more precisely the anomalous behaviour of intensities at a distance of 60–120 km observed in many intensity prediction studies (Somerville and Yoshimura 1990; Gasperini 2001) among others. This fact is of extraordinary importance in the characterization of seismic hazard.

2 Seismic-intensity data collection in continental Spain and the Balearic Islands

In recent years, several different collations of intensity data have been performed for earthquakes in Spain and nearby countries such as Portugal, France and Morocco. In Spain, the first studies of earthquake intensities consisted of data collation by Galbis (1932, 1940), Rey Pastor (1949) and Fontserè and Iglésies (1971). From 1964 to 1990, the Instituto Geográfico Nacional published in their seismological bulletins all available macroseismic information in the form of isoseismal maps. For the period 1995–1997, the seismic bulletins contain a list of the localities in which earthquakes were felt, along with their associated intensities all of which were included in the revision by Mezcua et al. (2013). From 1998 to the present day, the IGN/SIS catalogue provides macroseismic information given with a list of time arrivals for each shock. The macroseismic scale used in this catalogue is the EMS-98 (Grünthal 1998), which is generally employed for assigning seismic intensities in European countries. It is characterized by its robustness, the rejection of any intensity correction due to soil conditions and the understanding that each IDP represents a village or town rather than being assigned to a particular point.

The first attempt to collate available information in the form of isoseismal maps was performed by Mezcua (1982). In this catalogue, a collection of 261 isoseismal maps was drawn up for the period 1396–1981. This intensity data was included in the *Sismicidad del Área Ibero-Mogrebí* (Mezcua and Martínez Solares 1983), while for the northeast of the Iberian Peninsula, a revision of the macroseismic data for events was published by Susagna (1999). In this catalogue, a total of 859 shocks—for which there is macroseismic information (MSK scale) for 601—occurring in the period 880 BC–1996 AD were revised. The events considered for the dataset used in this paper were converted to the EMS-98 scale using the relationship between the two scales (Musson et al. 2010).

A full revision of all available information for 880 BC–1900 AD was collated by Martínez Solares and Mezcua (2002) in their catalogue of seismic activity in the Iberian Peninsula. A total of 2311 events were catalogued, far more than the 1181 events previously cited for this period in the official catalogue. In this study, the EMS-98 scale was applied in the description of each event. This catalogue is included in the Archive of Historical Earthquake Data (AHEAD) as part of the project Network of Research Infrastructures for European Seismology (NERIES), which also includes a revision for Catalonia (NE Spain) (Olivera et al. 2006). For the French border of the Pyrenees, the SISFRANCE-BRGM-EDF-IRSN (2010) catalogue was also consulted and the corresponding information added.

More recently, Mezcua et al. (2013) compiled intensity data points for 163 events with maximum intensity 5 or greater for Spain, which includes 39 events studied by Mezcua et al. (2004) for which an IPE was calculated.

Since 2008, the Instituto Geográfico Nacional (IGN) has collated the intensities of earthquakes via the Internet. The *Did you feel it?* method (DYFI) developed by Dengler and Dewey (1998), calibrated to give an MMI as an output (Wald et al. 1999), was adapted by Rueda and Mezcua (2011) for Spain. This automated intensity information given in terms of the Modified Mercalli intensity and is available for each earthquake in the form of a list of sites with their assigned intensity values. The intermediate degrees obtained from this method are rounded to the nearest half integer and added to the intensity file. This information is converted to the EMS-98 scale using the equivalence given by Musson et al. (2010) and forms part of the reference data associated with each earthquake in the IGN/SIS catalogue for Spain.

The intensity databank used in this paper was obtained by merging the four most recent intensity files described above (Fig. 1) and the spatial distribution of the epicentres they contain (Fig. 2). The intensity information contained in this databank consist of 37,682 IDPs, corresponding to 5512 events for the Iberian Peninsula and southern France in the period up to 31 December 2018 (Fig. 3); in all, 55% are Internet-based IDPs and the remaining 45% obtained in the traditional way by applying of a macroseismic scale. This file contains the focal parameters of each shock, as well as the different parameters for each earthquake given in the literature and the coordinates and intensity values for each location where it was felt. We also include the site amplification factors for both the short- and midterm period obtained from the geological classification of the Iberian Peninsula and the Balearic Islands (Núñez et al. 2012), although they have not been applied in this paper. For each location, the epicentral and hypocentral distances are also given.

3 Intensity prediction equation for continental Spain

The intensity experienced from an earthquake varies with the distance from the origin of the shock and depends intrinsically on the geometrical spreading of the seismic wave front, their local amplification, the anelastic properties expressed in the quality factor of the media and the possible directivity effects that may be present. However, for hypocentral distances greater than 10–20 km, the effect of the geometrical spreading may be dominant. Consequently, the distance behaviour of the intensity permits an intensity to be assigned in

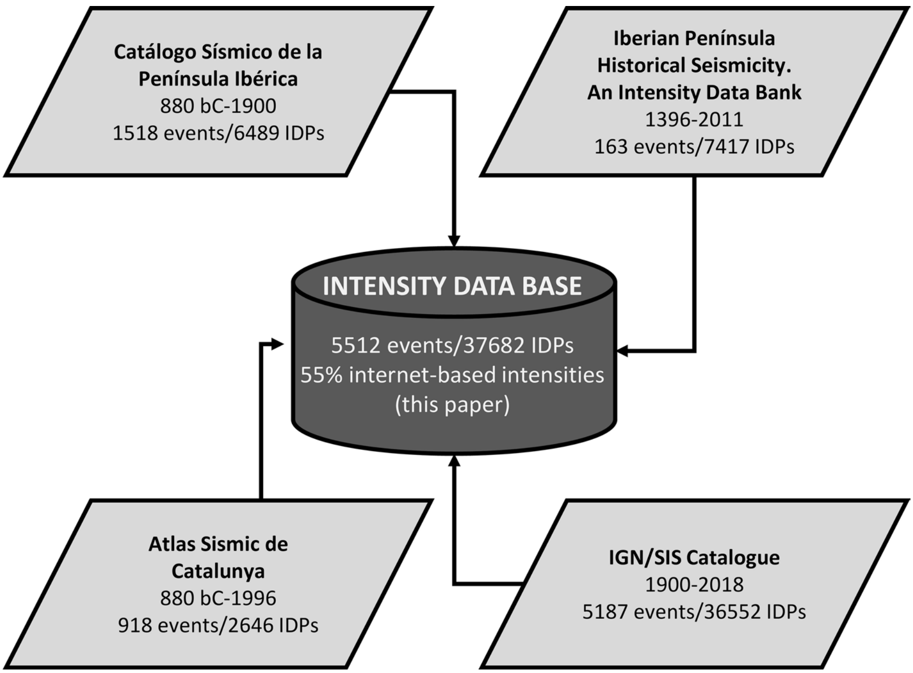

Fig. 1 The four different intensity data sets used for the compilation of the intensity databank presented in this paper. Statistics on the shocks and IDPs for each file are also given

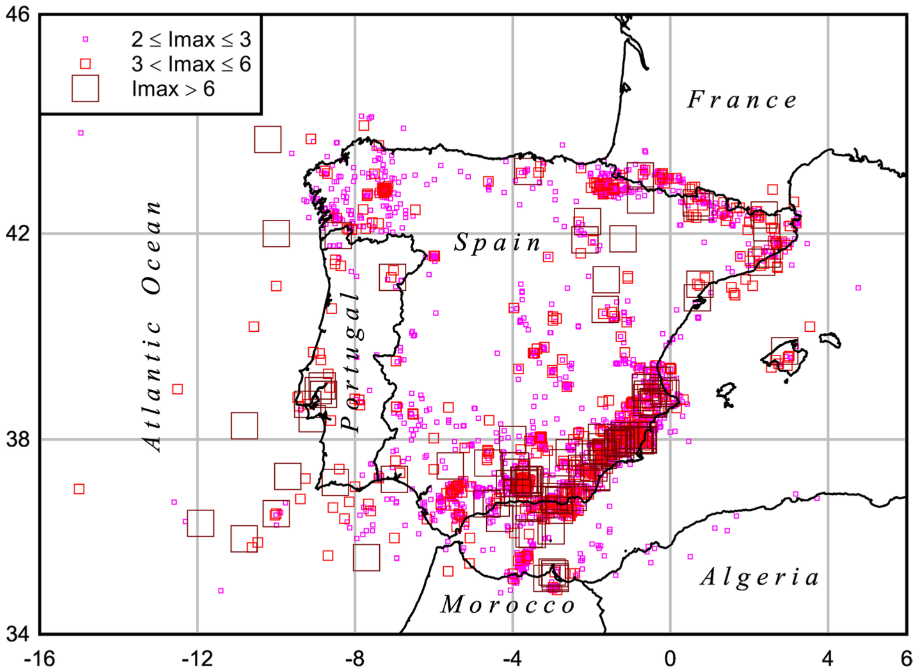

Fig. 2 Epicentres included in the intensity dataset used in this paper. The size of the symbol corresponds to the maximum intensity assigned to each shock

terms of the distance itself, the anelastic attenuation and the size of the event, represented by its moment magnitude. The resulting IPE is of great importance in intensity-based hazard studies.

The modelling of the intensity takes the form (Atkinson et al. 2014)

$$I = C_1 + C_2M + C_3R + C_4 \log R \quad (1)$$

where C_1 is the calibration parameter, C_2 represents the magnitude dependence, C_3 is the anelastic attenuation factor and C_4 is the geometrical spreading. R is the distance to the fault, which can be replaced by the hypocentral distance for small-to-moderate events (Atkinson and Wald 2007). We did not consider the transition distance term in the decay of the intensity with distance over a specific distance range (60–120 km approximately) (Atkinson and Wald 2007) due to the Moho reflections of the seismic waves (Burger et al. 1987). The reason is that this term is not well defined in terms of actual intensity data since, due to the low magnitude ($M < 5.1$) of the events in the Internet-based intensity databank, the corresponding intensities for this distance interval are low. For instance, for a magnitude 4 event, the corresponding intensity at this distance is around 2, a value that is not complete. Moreover, for the remaining data files with greater magnitudes in this distance interval, intensity data are scarce and also usually incomplete.

In order to obtain the four constants, in the intensity data file created for this paper, we considered 106 calibration events of which 105 were instrumental with an observed moment magnitude in the range 3.3–5.3, as well as one historical event, the Andalusian Earthquake of 1884 with a deduced moment magnitude of 6.4 (Mezcua et al. 2013). The

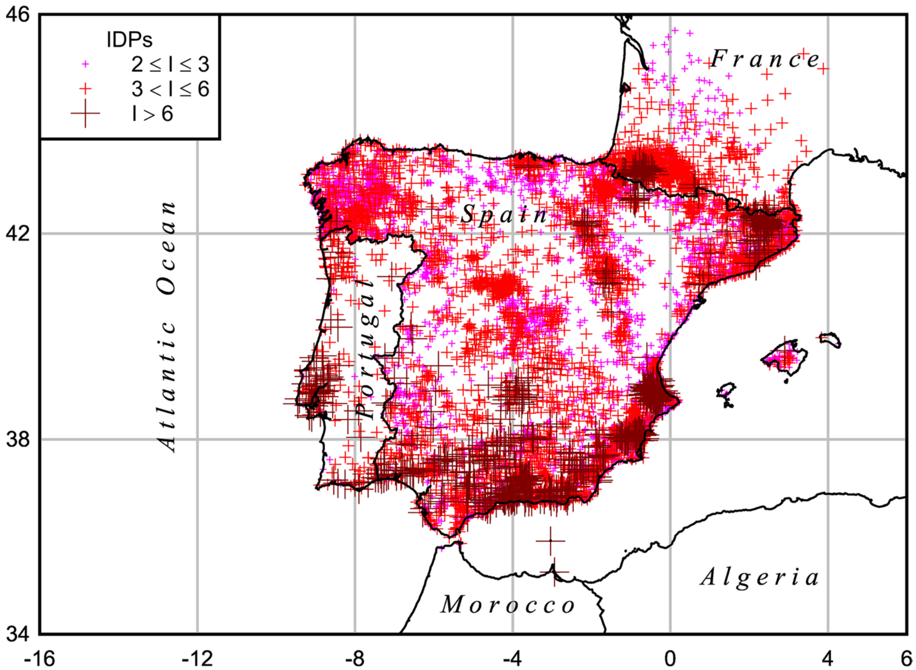

Fig. 3 Intensity data points registered in the intensity dataset. The size of the symbol corresponds to the maximum intensity at each location

observed values of intensity for these calibration events were binned into equally spaced log distance intervals of 0.2 log units in width (Fig. 4). The use of binned intensities enhances the weak intensity behaviour with distance. Intensity 2 was the minimum value considered.

In an attempt to regionalize this intensity prediction, we took into account for the Iberian Peninsula three main seismotectonic units defined for intensity attenuation by the EU Commission's SHARE project of seismic hazard harmonization in Europe (Delavaud et al. 2012): a Stable Continental Region (SCR), the Western Alps and Pyrenees and the Betic region. The SCR is characterized by Precambrian crystalline igneous rocks with low attenuation and a low deformation rate (Capote et al. 2002; González-Drigo et al. 2003), while the Betic region constitutes an alpine arch-shaped thrust belt with a crystalline basement and sedimentary cover with different tectonic units of Paleaozoic and Triassic rocks and the Guadalquivir basin filled with Neogene deposits, showing high attenuation and deformation rate (Saenz de Galdeano and Vera 1992; González-Drigo et al. 2003). The Pyrenees is an orogenic belt between France and Spain resulting from an incipient underthrusting of the Iberia crust under Europe that consists largely of granite and gneiss rocks with very low wave attenuation (González-Drigo et al. 2003). The distribution of the calibration events for each zone is as follows: the Pyrenees 26 shocks and 2557 IDPs including the French data for the 13 August 1967 Arette Earthquake of $M = 5.3$ (SISFRANCE-BRGM-EDF-IRSN 2010); SCR with 34 shocks and 3756 IDPs and Betic 46 events and 4252 IDPs. Besides the epicentre included in each zone, the selection criteria were (1) shallow depths of less than 20 km and (2) a moment magnitude calculated or by converting the

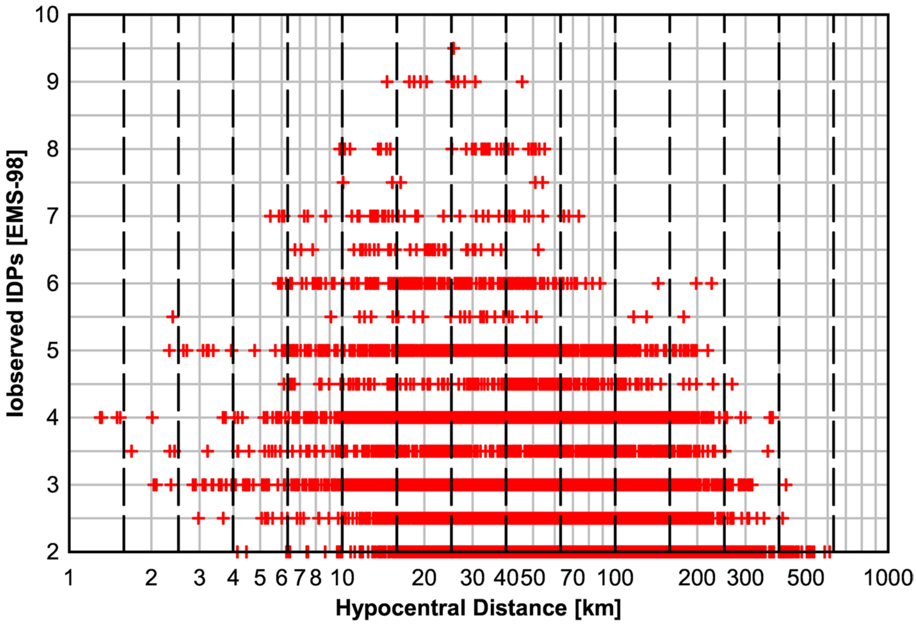

Fig. 4 IDPs for the 106 calibration events showing the equally spaced log distance intervals of 0.2 log units in width

corresponding magnitude provided by Cabañas et al. (2015). These three units are shown in Fig. 5, along with the calibration events selected for each zone.

A least squares regression of Eq. 1 applied to each individual seismotectonic zone and their sum (i.e. the Spanish mainland) give the following results:

$$\text{Spain} \quad I = -0.616 + 1.528\,M - 0.0022R - 1.544\log R \quad \sigma = 0.62 \tag{2}$$

$$\text{Betics} \quad I = -0.115 + 1.553\,M - 0.0011R - 1.994\log R \quad \sigma = 0.60 \tag{3}$$

$$\text{Pyrenees} \quad I = -2.559 + 1.774\,M - 0.0062R - 0.933\log R \quad \sigma = 0.60 \tag{4}$$

$$\text{SCR} \quad I = -0.223 + 1.347\,M - 0.0023R - 1.235\log R \quad \sigma = 0.59 \tag{5}$$

These prediction equations provide an average intensity as a function of moment magnitude preferable in the 3.5–6.0 magnitude range and the closest distance to the fault (10–180 km), which is equivalent to the hypocentral distance for the magnitude range considered. These equations for $M = 4$, 5 and 6 are shown in Fig. 6. From this figure, we may observe that from 20 km onwards and magnitudes 5 and 6, there is small difference between the three zones and the resulting value for Spain, being the Pyrenees IPE with a very small geometrical spreading coefficient (0.933) the slower from this distance up to 180 km approximately.

To check how the deduced IPEs for Spain represent the data, the residuals of the observed minus the calculated intensity values versus the binned distances used to derive this equation are represented in Fig. 7. In this graph, we include the standard deviation of the residuals for each distance interval. Only the first three intensity bins corresponding to

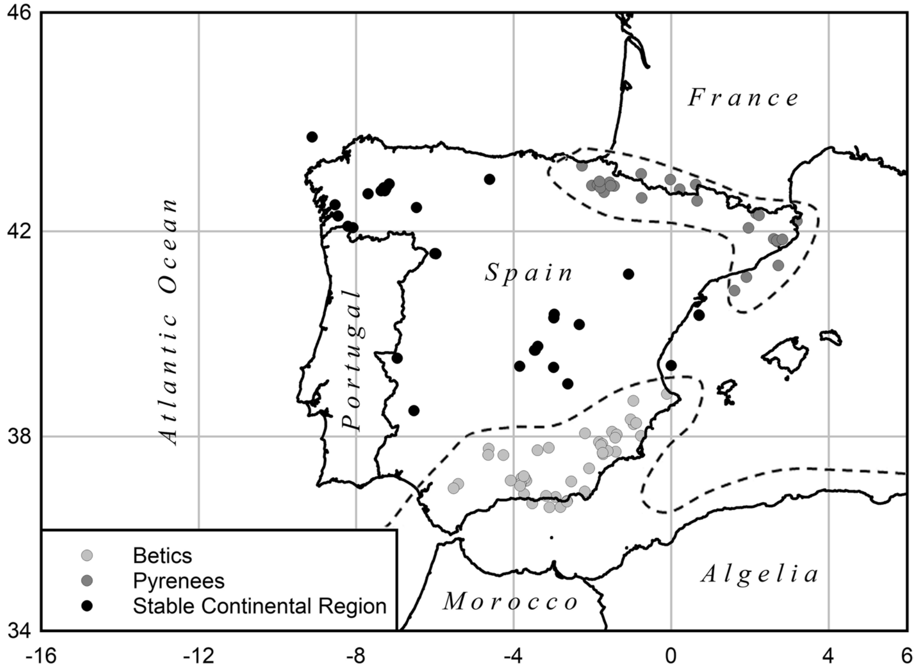

Fig. 5 Epicentres of shocks used in the regression for each of the seismotectonic Iberian units according to Delavaud et al. (2012)

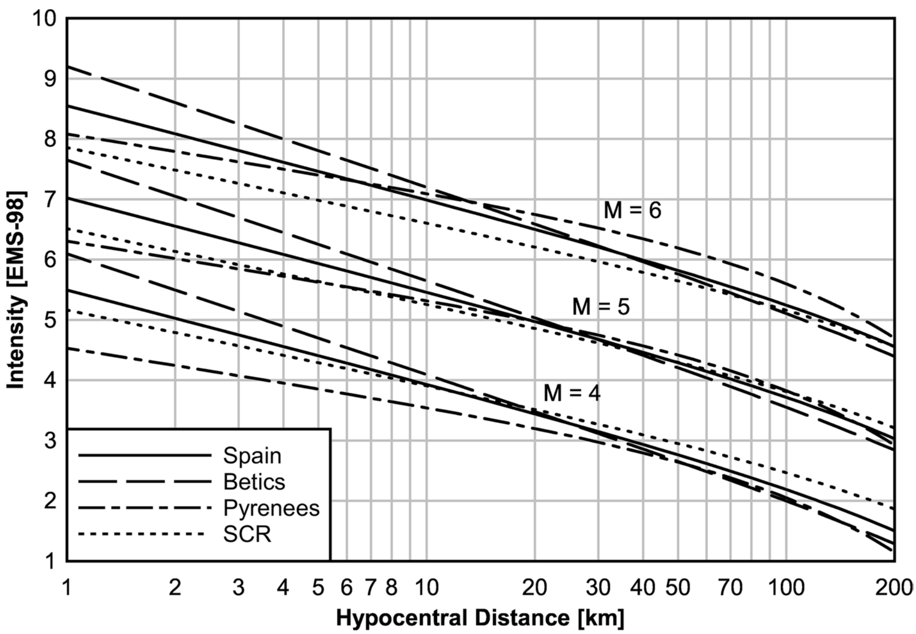

Fig. 6 Deduced intensity prediction equations (IPE) corresponding to each seismotectonic unit and to Spain for magnitudes M 4, 5 and 6

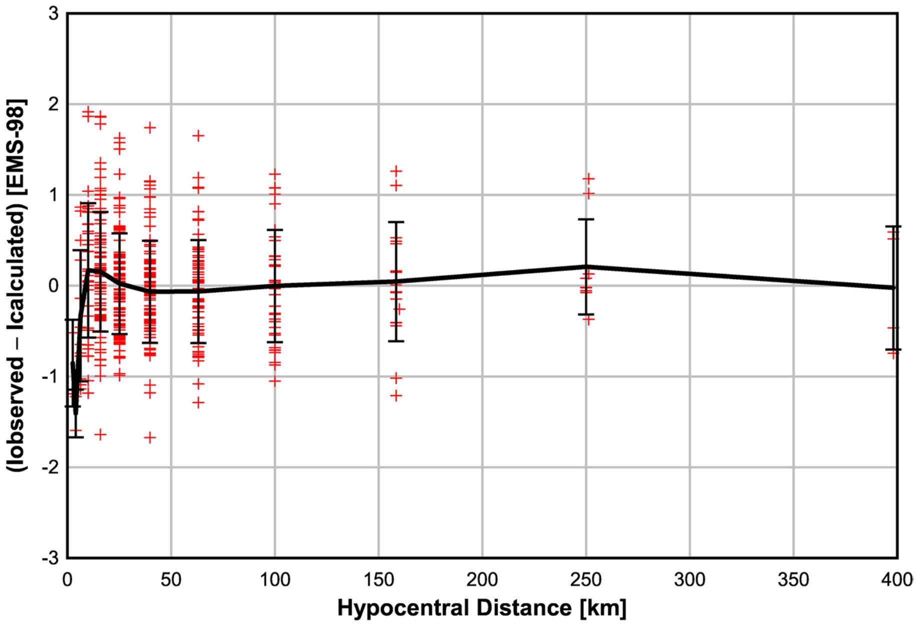

Fig. 7 Observed minus calculated intensity values for Spain of the IDPs used in the regression. Observed intensity values were binned into equally log distance intervals of 0.2 log units in width, representing also their mean value and its standard deviation

the 0–10 km hypocentral distance shows negative residuals where the influence of the local geology and other source effects, together with the possible lack of depth control, may be responsible for these variations which shows that the IPE overestimates the intensity values. Beyond this distance, residuals are above and close to zero showing a weak increase up to a distance of 250 km.

To compare the behaviour of this equation with the total intensity file, we show in Fig. 8 the residuals for the IDPs in the range 5–200 km for 2010–2018, which can be assumed to be homogeneous. The residual in this distance range can be divided for the different hypocentral distances into three stages: a positive residual decreasing down to zero in the first 65 km, an increase in the residual in the 70–125 km distance range, and lastly, a negative residual in the 130–225 km range.

Finally, a histogram of the residuals for the total intensity databank is shown in Fig. 9, showing a normal distribution with a standard deviation of 0.89 and a maximum around zero. Most of the residuals are in the $(-2.0, +2.0)$ of intensity.

4 Comparison with other intensity prediction equations

Recently, France and Portugal have developed IPEs based on the moment magnitude, and a comparison is shown in Fig. 10. Given that the Portuguese relationship, Le Goof et al. (2014) defined in terms of the epicentral distance, we consider a focal depth of 10 km to be able to compare results. The Spanish IPE is more attenuated than those of the two other countries in the close distance range of <20 km. However, beyond this distance the

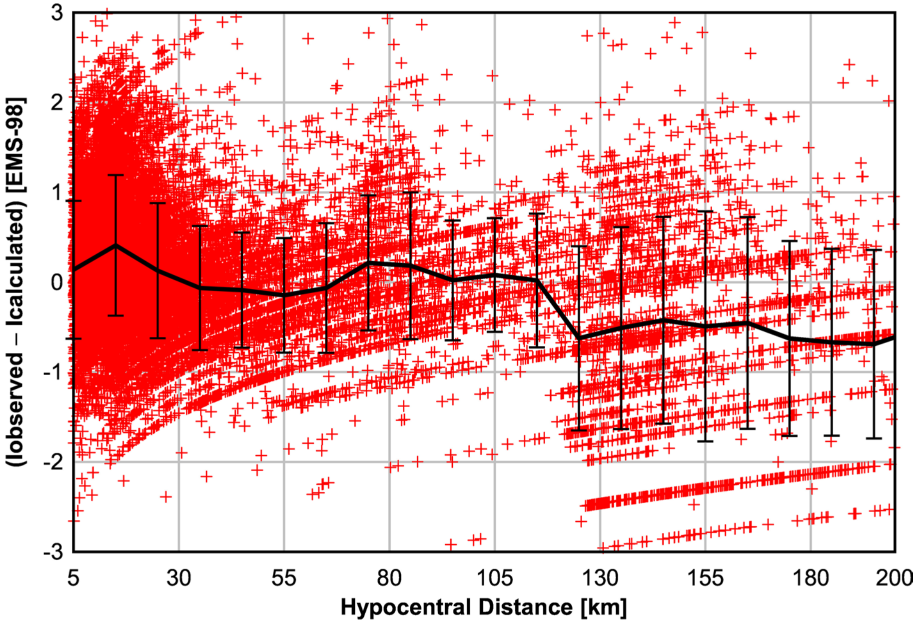

Fig. 8 Observed minus calculated intensity values for Spain of the IDPs of the intensity dataset in the 5–200 km range for the period 2010–2018. Intensity bins for each 10-km distance interval is also represented with its standard deviation

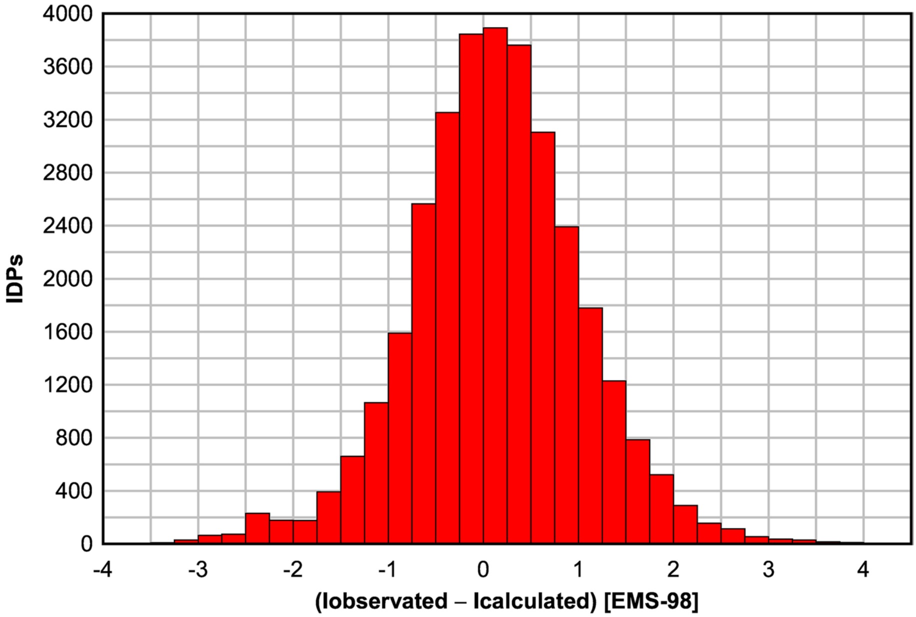

Fig. 9 Histogram of the differences in the observed minus calculated intensity values for Spain for the whole intensity dataset

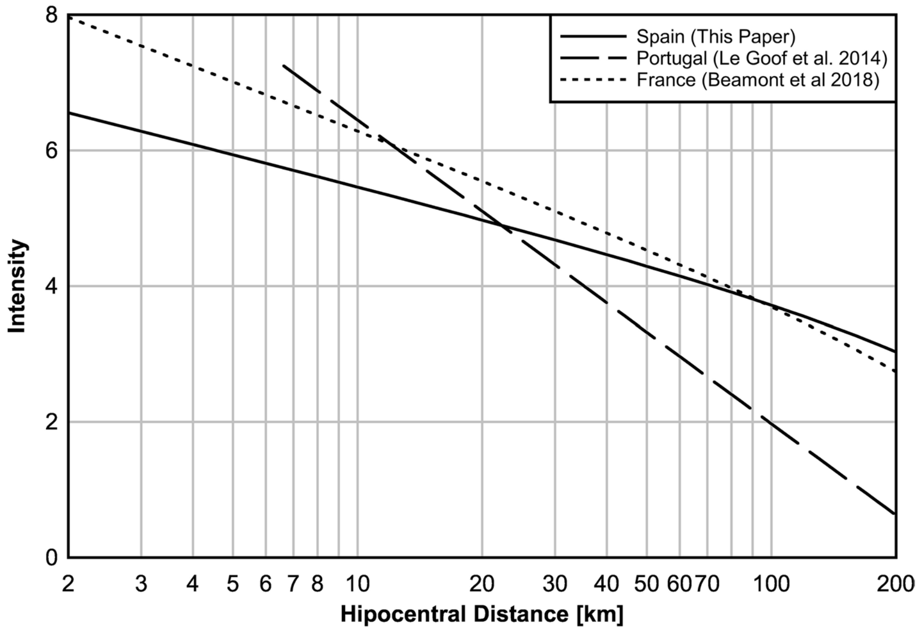

Fig. 10 Comparison between the IPEs corresponding to $M=5$ for Portugal (Le Goof et al. 2014) and Metropolitan France (Baumont et al. 2018), and the result for Spain given in this paper

French and Spanish relationships converge at 90 km, the point at which the latter becomes less attenuated. The French IPE considered here was recently published by Baumont et al. (2018). For Portugal, the IPE is almost two intensity units more attenuated than the French and Spanish IPEs at a distance of 100 km. The reason for this difference may be due to the incomplete datasets used in the Portuguese IPE (Le Goof et al. 2014) and, possibly, the use of earthquakes at greater depths corresponding to offshore events in the Gulf of Cádiz. Another important consequence of this comparison is that the greater Spanish attenuation in the range <20 km could be due to the scarcity of IDPs in the dataset for this range. The coefficients that represent the geometrical spreading value for Spain obtained in this paper is lower (1.546) than the obtained (2.793) in the project NERIES for Iberia (Stucchi et al. 2010) and also the anelastic coefficient (0.0022) against the (0.0036) of the same project. However, those parameters for Spain as compared with the corresponding to Continental France with values (2.376) and (0.0023), respectively, are in better agreement.

5 Intensity signature at an intermediate (60–130 km) distance range

A number of intensity distance studies have noted that anomalous behaviour occurs at distances from the epicentre in the range, approximately, of 60–130 km (Atkinson and Wald 2007; Atkinson et al. 2014) due to the Moho bounce of the post-critical reflections and refractions combined with the direct train of waves (Burger et al. 1987). As mentioned above, we aimed to introduce a term into the IPE to attempt to identify this behaviour in the Spanish IPE. Unfortunately, not enough data were available in this distance range to reproduce this phenomenon. We tried to investigate whether or not this anomaly is present when a large amount of data for this distance range is available by comparing both the observed and the predicted values in order to quantify the precise distance range. The differences between the binned hypocentral distance intensity values at a 10 km interval for the intensity file in 2009–2018 and their standard deviations from the values deduced from the Spanish IPEs are shown in Fig. 11. The median value is positive for 0–30 km and then is slightly negative up to 55 km. From this point onwards, the differences between the observed binned intensities minus the calculated values increases to positive values up to 120 km. From this distance up to a limit around 200 km, attenuations of a similar tendency to that observed in the first interval reoccur, albeit with greater negative values. In order to explain the anomalous behaviour of the observed differences, we considered a crust model for the Iberian Peninsula (Mezcua and Martínez Solares 1983) used for routine earthquake location by the Instituto Geográfico Nacional of Spain. This model consists of two-layer crust and a Moho depth of 30 km. However, in the central Betic, the Moho may reach 38 km, Banda et al. (1993) and around 40 km for the Pyrennes belt, Diaz et al. (2016). With this average Moho depth, a Moho bounce is expected to occur in the 60–120 km interval, which may vary depending on the focal depth (Burger et al. 1987). We can conclude that the observed intensity differences values in the 60–120 km range are relatively higher than the two adjacent intervals, which we interpret as being a consequence of the Moho bounce of the waves combined with the direct waves.

In order to check whether or not this result can be confirmed by the direct observation of the amplitude decay of waves related to the intensity, we took into account the amplitude decay of the PGV observed for the area. We selected 11 events occurring on the Spanish mainland that have been recorded in the Spanish broadband network. The parameters of

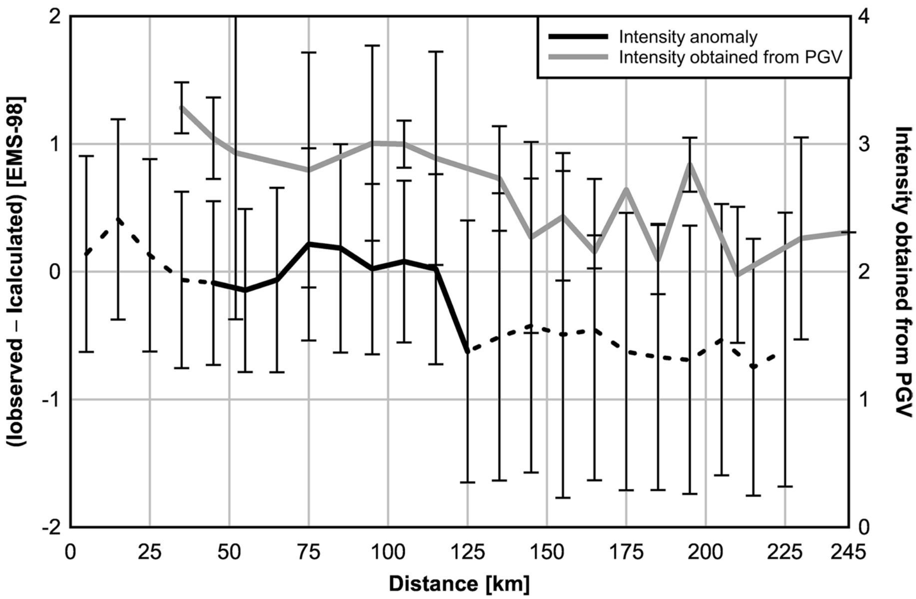

Fig. 11 Observed minus calculated intensities as a function of hypocentral distance for the Spanish IDPs for the 2009–2018 intensity databank (black line). Theoretical intensity obtained from the PGV of 11 events recorded in the Spanish Broadband Seismic Network (grey line) as a function of corresponding hypocentral distances

these events in the moment magnitude range (4.5–5.1) are given in Table 1. The PGV values have been converted to intensity using the relationship proposed for intraplate events in eastern North America (Dangkua and Cramer 2011), given the similarity in its crust structure and tectonic regime. The resulting theoretical intensities obtained from each of the 82 PGV values for the 34–250 km interval were binned at 10 km intervals and are represented together with their standard deviation. It becomes clear that the theoretical intensity decays up to almost 75 km is followed by an increase in the intensity up to 135 km, with an average attenuation close to the R^0 expected for a Moho bounce. From that distance onwards, the intensity decay changes to $R^{-0.2}$. The coincidence in the anomalous behaviour of both variables, the difference in the intensity observed minus calculated values, and the theoretical intensity obtained from the observed PGV decay in the same distance range strongly suggests that, in the 60–120 km distance interval, the proposed IPE underestimates the values of intensity due to the Moho-bounce effect.

6 Results and conclusions

We compiled an intensity dataset from different sources of which the four most important sources in terms of the amount of data were Martínez Solares and Mezcua (2002), Mezcua et al. (2013), Susagna (1999) and the IGN/SIS catalogue of the Instituto Geográfico Nacional of Spain which is currently collating data via the Internet. In this compilation, published studies of historical events were also included, with new data substituting old data or being added.

The IPEs are associated with the three different seismotectonic areas into which the Spanish mainland can be divided. The resulting IPEs show that the Pyrenees unit provides the greatest intensities in a range 20–180 km for $M=4$ and 5, while the Betics IPE provides the lowest intensities in this distance range. However, for distances up to 20 km, the Betic IPE is less attenuated than the Pyrenees and SCR zones. The intensity differences between the three IPEs at long distance have an order of intensity degree of less than 0.5. An IPE for Spain can be calculated by combining data from the three regions to give an average relationship. The comparison with nearby countries reveals that the IPE for Spain in the

Table 1 Characteristics of the earthquakes used to obtain the PGV values recorded in the Spanish Broadband Seismic Network

Date	Latitude°	Longitude°	Depth (km)	*M*	Location
4 February 2002	37.0931	−2.5379	1	4.6	Gérgal (Almería)
6 August 2002	37.8925	−1.8353	1	5.0	Bullas (Murcia)
18 September 2004	42.8508	−1.4506	7	4.5	Lizoáin (Navarra)
29 January 2005	37.8535	−1.7555	11	4.8	Aledo (Murcia)
17 November 2006	43.0274	0.0150	0	4.5	Lourdes (Francia)
12 August 2007	39.3743	−2.9894	16	4.7	Pedro Muñoz (Ciudad Real)
2 October 2008	37.0442	−5.4112	8	4.7	Coripe (Sevilla)
11 May 2011	37.7175	−1.7114	4	5.1	Lorca (Murcia)
11 May 2011	37.7196	−1.7076	2	4.5	Lorca (Murcia)
23 February 2015	39.0475	−2.6273	17	4.7	Ossa de Montiel (Albacete)
21 January 2016	35.6385	−3.7951	0	5.1	Alborán Sea

0–25 km distance interval provides the smallest intensities, while the interval between 25 km and around 70 km lies between the intensity corresponding to Portugal and France. However, in the distance interval 90–180 km, the Spanish IPE is the least attenuated of all three countries.

Finally, we also observed different intensity decay in the 60–120 km interval in which the corresponding intensity values are underestimated by our relationship. This may be caused by the constructive interference of direct, reflected or refracted waves at the Moho (Moho bounce). This anomaly is also confirmed by the similar behaviour of the theoretical intensity obtained from the PGV values of 11 recorded events in the Spanish broadband network.

7 Data and resources

Most of the intensity data used in this study are freely available from the Instituto Geográfico Nacional of Spain. The four intensity data files used in this paper are: Catalogo Sísmico de la Península Ibérica 880 bC-1900., Martínez Solares and Mezcua (2002) (https://www.ign.es/web/resources/sismologia/publicaciones/Catalogohasta1900.pdf, last accessed, January 2019); Atlas seismic de Catalunya 880 bC-1996., Susagna (1999) (https://www.igc.cat/web/files/atles_sismic.pdf, last accessed, March 2019; the IGN/SIS Catalogue. 1900–2018., IGN Intensity Data File (https://www.ign.es/web/ign/portal/sis-catalogo-terremotos, last accessed, January 2019); and SISFRANCE-BRGM-EDF-IRSN/SisFrance (2010) (https://www.sisfrance.net, last update September 2015).

Acknowledgements The authors sincerely acknowledge the thoughtful comments and careful revision of R. Musson and J.A. Peláez which helped substantially to improve our original manuscript enhancing their quality. We are also grateful to Michael Lockwood who proofread the English and Marta García Vargas for editing the intensity database used in this work.

Compliance with ethical standards

Conflict of interest The authors declare that they have no conflict of interest.

References

Atkinson GM, Wald DJ (2007) "Did you feel it?" Intensity data: a surprisingly good measure of earthquake ground motion. Seismol Res Lett 78:362–368

Atkinson G, Worden CB, Wald DJ (2014) Intensity prediction equations for North America. Bull Seismol Soc Am 104:3084–3093

Bakun WH, Wentworth CM (1997) Estimating earthquake location and magnitude from seismic intensity data. Bull Seismol Soc Am 87:1502–1521

Bakun WH, Scotti O (2006) Regional intensity attenuation models for France and the estimation of magnitude and location of historical earthquakes. Geophys J Int 164:596–610

Banda E, Gallart J, García-Dueñas J, Dañobeitia JJ, Makris J (1993) Lateral variation of the crust in the Iberian Peninsula: new evidence from the Betic Cordillera. Tectonophysics 221:53–66

Baumont D, Manchuel K, Traversa P, Durouchoux C, Nayman E, Ameri G (2018) Intensity predictive attenuation models calibrated in Mw for metropolitan France. Bull Earthq Eng 16:2285–2310

Bonelli J, Esteban Carrasco L (1957) El sismo destructor de 19 de abril de 1956 en la región de Granada. Revta Geofís XVI, vol 61 **(in Spanish)**

Burger R, Somerville P, Barker J, Herrmann R, Helmberger D (1987) The effect of crustal structure on strong ground motion attenuation relations in eastern North America. Bull Seismol Soc Am 77:420–439

Cabañas L, Rivas-Medina A, Martínez Solares JM, Gaspar Escribano JM, Benito B, Antón R, Ruiz Barajas S (2015) Relationships between Mw and other earthquake size parameters in the Spanish IGN Seismic Catalog. Pure Appl Geophys 172:2397–2410

Capote R, Antón JA, Simón JL, Liesa CL, Arlegui LE (2002) Alpine tectonics I: the alpine System north of the Betic cordillera in the Geology of Spain. In: Gibbons W, Moreno T (eds) The Geological Society of London Special Publications, pp 368–400

D'Amico V, Albarello D (2008) SASHA: a computer program to assess seismic hazard from intensity data. Seismol Res Lett 79:663–671

Dangkua D, Cramer CH (2011) Felt intensity versus instrumental ground motion: a difference between California and Eastern North America? Bull Seismol Soc Am 101:1847–1858. https://doi.org/10.1785/0120100133

Delavaud E, Cotton F, Akkar S, Scherbaum F, Danciu L, Beauval C, Drouet S, Douglas J, Basili R, Sandikkaya MA et al (2012) Toward a ground-motion logic tree for probabilistic seismic hazard assessment in Europe. J Seismol 16:451–473. https://doi.org/10.1007/s10950-012-9281-z

Dengler LA, Dewey JW (1998) An intensity survey of households by the Northridge, California, earthquake of 17 January 1994. Bull Seismol Soc Am 88:441–462

Diaz J, Gallart J, Carbonell R (2016) Moho topography beneath the Iberian-western Mediterranean region mapped from controlled-source and natural seismicity surveys. Tectonophysics 692:74–85

Fontserè E, Iglésies J (1971) Recopilació de dades sísmiques de les terres catalanes entre 1100 i 1906. Fundació Salvador Vives i Casajuana. Barcelona **(in Catalan)**

Galbis J (1932) Catálogo Sísmico de la zona comprendida entre los meridianos 5° E y 20° W de Greenwich y los paralelos 45° y 25° N. Tomo I. Instituto Geográfico y Catastral **(in Spanish)**

Galbis J (1940) Catálogo Sísmico de la Zona Comprendida entre los meridianos 5° E y 20° W y los paralelos 45° y 25° N. Instituto Geográfico y Catastral. Tomo II **(in Spanish)**

Gasperini P (2001) The attenuation of seismic intensity in Italy: a bilinear shape indicates the dominance of deep phases at epicentral distances longer than 45 km. Bull Seismol Soc Am 91:826–841. https://doi.org/10.1785/0120000066

Gasperini P, Bernardini F, Valensise G, Boschi E (1999) Defining seismogenic sources from historical earthquake felt reports. Bull Seismol Soc Am 89:94–110

Gómez-Capera AA, Rovida A, Gasperini P, Stucchi M, Vigand D (2015) The determination of earthquake location and magnitude from macroseismic data in Europe. Bull Earthq Eng 13:1249–1280. https://doi.org/10.1007/s10518-014-9672-3

González-Drigo R, Pujades L, Caselles O, Canas JA (2003) Distribución de Q de coda y análisis de la atenuación sísmica intrínseca y dispersiva en la Península Ibérica. Rev Int Mét Num Cal Dis Ing 19:211–237 **(in Spanish)**

Goula X, Dominique P, Colas B, Jara JA, Roca A, Winter T (2008) Seismic rapid response system in the Eastern Pyrenees. In: XIV world conference on earthquake engineering. Beijing, China

Grünthal G (ed) (1998) European Macroseismic Scale 1998. Cahiers du Centre Europèen de Gèodynamique et de Seismologie. Conseil de l'Europe, Conseil de l'Europe, vol 15

Hough S (2013) Spatial variability of "Did you feel it?" Intensity data: Insights into sampling biases in historical earthquake intensity distributions. Bull Seismol Soc Am 103:2767–2781

Inglada V (1921) Nuevas fórmulas para abreviar el cálculo de la profundidad aproximada del foco sísmico por el método de Kövesligethy y su aplicación a algunos temblores de tierra. Instituto Geográfico y Estadístico, Madrid **(in Spanish)**

Kövesligethy RD (1906) A makroszeizmikus rengések feldolgozása. Mathematikai és Természettudományi Értesítõ 24:349–368 **(in German)**

Le Goof B, Borges JF, Bezzeghoud M (2014) Intensity-distance attenuation laws for the Portugal mainland using intensity data points. Geophys J Int 199:1278–1285. https://doi.org/10.1093/gji/ggu317

López Casado C, Molina S, Delgado J, Peláez JA (2000) Attenuation of intensity with epicentral distance in the Iberian Peninsula. Bull Seismol Soc Am 90:34–47

Mak S, Schorlemmer D (2016) A comparison between the forecast by the United States National Seismic Hazard Maps with recent ground-motion records. Bull Seismol Soc Am 106:1817–1831. https://doi.org/10.1785/0120150323

Mak S, Clements RA, Schorlemmer D (2015) Validating intensity prediction equations for Italy by observations. Bull Seismol Soc Am 105:2942–2954. https://doi.org/10.1785/0120150070

Martín AJ (1984) Riesgo sísmico en la Península Ibérica. PhD Thesis. Instituto Geográfico Nacional, Madrid, vol 2 **(in Spanish)**

Martínez Solares JM, Mezcua J (2002) Catálogo Sísmico de la Península Ibérica (800 a.C.-1900). Monografía N°. 18. Instituto Geográfico Nacional **(in Spanish)**
Mezcua J (1982) Catálogo General de Isosistas de la Península Ibérica. Publicación 202. Instituto Geográfico Nacional. Madrid **(in Spanish)**
Mezcua J, Martínez Solares JM (1983) Sismicidad del Área Ibero-Mogrebí. Publicación 203. Instituto Geográfico Nacional. Madrid **(in Spanish)**
Mezcua J, Rueda J, García Blanco RM (2004) Reevaluation of historic earthquakes in Spain. Seismol Res Lett 75:75–81
Mezcua J, Rueda J, García Blanco RM (2013) Iberian Peninsula historical seismicity revisited: an intensity data Bank. Seismol Res Lett 84:9–18
Muñoz D (1983) Estudio del Riesgo Sísmico en el Sur y Sureste de la Península Ibérica. Tesis Doctoral, Universidad Complutense de Madrid (**in Spanish**)
Musson RMW (2005) Intensity attenuation in the UK.". J Seismol 9:73–86
Musson RMW, Jiménez MJ (2008) Macroseismic estimation of earthquake parameters. NA4 deliverable D3, NERIES Project. https://emidius.mi.ingv.it/neries_NA4/deliverables. Last accessed January 2015
Musson RMW, Grünthal G, Stucchi M (2010) The comparison of macroseismic intensity scales. J Seismol 14:413–428. https://doi.org/10.1007/s10950-009-9172-0
Nuñez A, Rueda J, Mezcua J (2012) A site amplification factor map of the Iberian Peninsula and the Balearic Islands. Nat Hazards 65:461–476
Olivera C, Redondo E, Lambert J, Riera JA, Roca A (2006) Els terratrèmols dels segles XIV i XV a Catalunya. Barcelona-ICC 2006. ISBN 84-393-6961-1 **(in Catalan)**
Rey Pastor A (1949) La comarca sísmica de Caravaca y el sismo de 23 de junio de 1948. Instituto Geográfico y Catastral **(in Spanish)**
Romero J, Bonelli JM (1951) La Erupción del Nambroque (junio-agosto de 1949). Comisión Nacional de Geodesia y Geofísica. Instituto Geográfico y Catastral **(in Spanish)**
Rueda J, Mezcua J (2011) Redes de medida y tratamiento de la Información Sísmica. Evaluación automática de la Intensidad Sísmica. En Jornadas Protección Civil: Modelos de Simulación Aplicados al Análisis de Riesgo Sísmico. Madrid noviembre de 2011 **(in Spanish)**
Sanz de Galdeano C, Vera JA (1992) Stratigraphic record and paleogeographical context of the Neogene basins in the Betic Cordillera, Spain. Basin Res 4:21–36
SISFRANCE-BRGM-EDF-IRSN/SisFrance (2010) Histoire et caractéristiques des séismes ressentis en France. https://www.sisfrance.net. Last update 01 Mar 2016. **(in French)**
Somerville P, Yoshimura J (1990) The influence of critical Moho reflections on strong ground motions recorded in San Francisco and Oakland during the 1989 Loma Prieta earthquake. Geophys Res Lett 17:1203–1206. https://doi.org/10.1029/GL017i008p01203
Stromeyer D, Grünthal G (2009) Attenuation relationship of macroseismic intensities in central Europe. Bull Seismol Soc Am 99:554–565
Stucchi M, Rovida A, Gomez Capera AA, Musson R, Papaioannou Ch, Batllo J with the collaboration of: Locati M, Albini P, Mirto C, Viganò D, Cassera A, Roca A, Tatevossian R (2010) European Earthquake Catalogue (1000–1963), M %3e 5.8. Deliverable D10. NEtwork of Research Infrastructures for European Seismology (NERIES). https://emidius.mi.ingv.it/neries_NA4/docs/NA4_D10.pdf. Last accessed January 2015
Susagna T (1999) Atles sismic de Catalunya. Volume 1. Catáleg de Sismicitat. Inst. Cartographic Catalunya **(in Catalan)**
Wald D, Quitoriano V, Dengler L, Dewey J (1999) Utilization of the Internet for rapid community intensity maps. Seismol Res Lett 70:680–697
White I, Liu T, Luco N, Liel AB (2018) Considerations in comparing the U.S. Geological Survey one-year induced seismicity hazard models with "Did You Feel It?" and instrumental data. Seismol Res Lett 89:127–137